C. RF System

1. Layout and General Parameters

The synchrotron radiation energy radiated by a 15 GeV electron circulating once around the PEP ring is 27 MeV. Additional energy is lost due to the excitation of parasitic modes in the RF structure itself, in vacuum chamber boxes, and at vacuum chamber discontinuities around the circumference of the ring, and this energy loss is calculated to be 3.7 MeV at a circulating current of 92 mA, based on assumptions to be discussed in detail later. In addition to restoring these losses, the RF accelerating cavities must provide an overvoltage in order to insure a useful quantum lifetime. At the PEP radiofrequency of 353 MHz (chosen for reasons to be discussed in the following section), a peak RF voltage of 49 MV is required for operation at 15 GeV with 92 mA stored in each beam.

A total of 9 MW is required and it is proposed that it be supplied by 18 klystrons, each delivering a cw output power of 500 kW. In the initial installation, each klystron will feed a single accelerating section 2.1 m in length. Each section comprises five coupled π-mode cavities very similar in design to the SPEAR II cavities. Six such accelerating sections will be located initially in each of Regions 4, 8, and 12. Within each of these regions, the layout of the sections may vary. In Region 12, present plans are to install a group of three sections on either side of the interaction point. In Regions 4 and 8, all six sections will be located on the B and A sides, respectively, of the interaction point. As shown in the layout of Fig. 28, the installation will be compatible with a future expansion of the RF system.

The initial complement of accelerating sections and vacuum pumps will be installed as shown by the solid-line components in Fig. 28. The RF system may

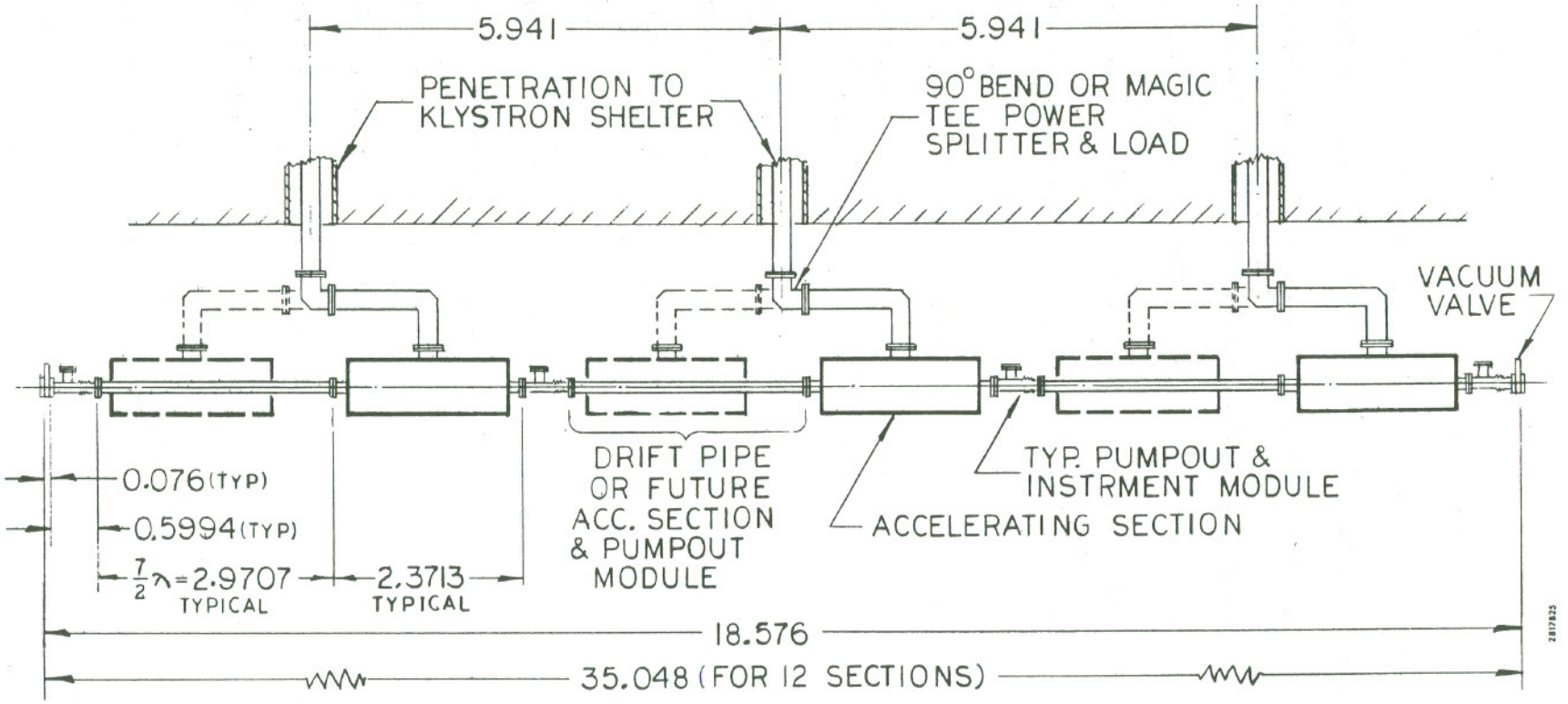

Fig. 28--RF cavity layout for Region 12. Cavity groups are twice as long in Regions 4 and 8.

be expanded at any time by increments of three additional accelerating sections so as to preserve symmetry around the ring. Orbit distortions due to either of these distributions of the RF cavities and synchrotron radiation loss have been calculated to be tolerable. As first constructed, drift pipes will occupy the spaces reserved for future accelerating sections. As these future sections are installed, a power splitter will replace the 90^{o} bend at the foot of the waveguide penetration so that each klystron will power two accelerating sections.

The plan for providing the RF system with the capability for ready future expansion, as shown by the layout in Fig. 28, represents an improvement over the RF system as originally proposed. Although the greater flexibility provided by this plan will occasion some additional expense, such as the cost of longer RF alcoves in the tunnel, compensating cost reductions have been achieved elsewhere in the system which will permit the overall cost to remain essentially the same as in the present cost estimate.

The klystrons will be housed in shelters above ground as shown in plan view in Fig. 29. An important feature of the construction is that the klystron power supplies are located on concrete pads outside the buildings. As shown in Fig. 30, waveguides running through vertical penetrations connect the klystrons to the accelerating sections in the tunnel below.

Typical parameters for the RF system at 15 GeV are shown in Table XIII, assuming a shunt impedance given by the measured shunt impedance for the SPEAR II cavities. The attainable circulating current depends strongly on the assumptions made concerning parasitic-mode losses in the RF cavities and vacuum chamber components. As discussed later in Section II.B.8, it is estimated that a parasitic-mode loss impedance of 40 MΩ can be attained at a bunch length of 4.5 cm (twice the natural bunch length). An impedance of this order will

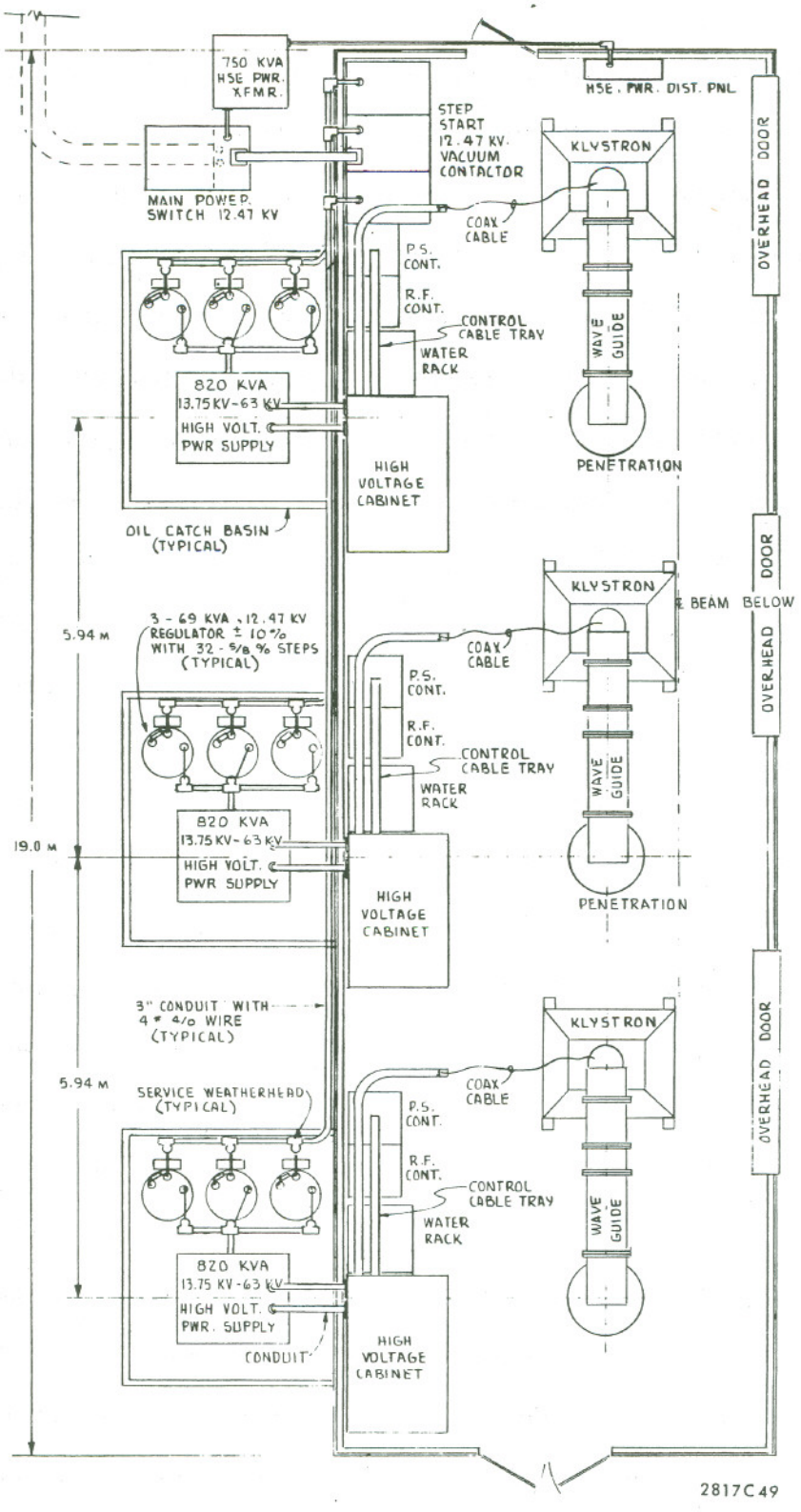

Fig. 29--Klystron housing in Region 12. In Regions 4 and 8 there are six klystrons per housing and each housing is twice as long.

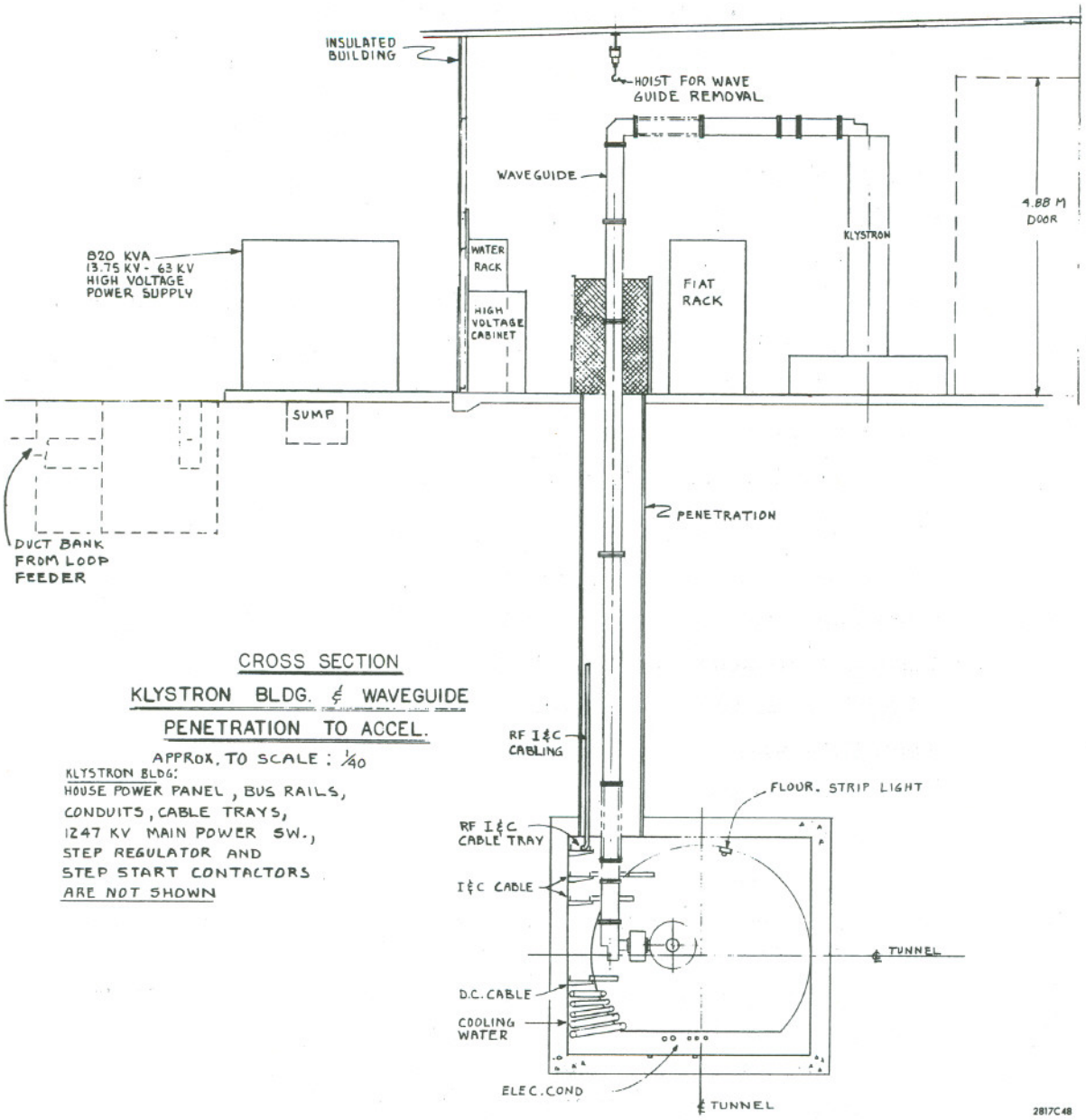

Fig. 30--RF penetration between klystron housing and tunnel.

TABLE XIII

Typical RF System Parameters at 15 GeV

Orbital Frequency	136.269	kHz
Harmonic Number	2592	
Frequency	353.209	MHz
Synchrotron Radiation Energy Loss per Turn	27.0	MeV
Higher-Mode Energy Loss per Turn[1]	3.7	MeV
Peak RF Voltage[2]	48.8	MV
Particles per Beam	4.2×10^{12}	
Circulating Current per Beam	92	mA
Synchrotron Radiation Power (both beams)	5.0	MW
Active Length of Accelerating Structure	38.2	m
Shunt Impedance for all Cavities Together[3]	715	MΩ
Fundamental-Mode Cavity Dissipation	3.3	MW
Power Loss to Parasitic Modes[1]	0.7	MW
Total RF Power	9.0	MW
Number of 500-kW Klystrons	18	
Total Power Input to RF Power Supplies	14	MW

[1] Estimated for a bunch length of 4.5 cm and a higher-mode loss impedance of 40 MΩ.

[2] For a quantum lifetime of 50 hours.

[3] The definition of shunt impedance used here is $R_s = V_p^2/P_c$, where R_s is shunt impedance, V_p is peak RF voltage and P_c is power dissipated in the cavity walls.

allow a circulating current of 92 mA per beam at 15 GeV. Since the parasitic-mode loss impedance depends on bunch length, the supportable circulating current will also depend on bunch length. There is no completely adequate theory which can give an exact prediction of the bunch lengthening to be expected in PEP. Consequently, bunch lengthening by a factor of two at 92 mA has been used in extrapolating SPEAR II results to the PEP case, using the potential-well-distortion model of bunch lengthening.[22] Should the bunch-lengthening factor be greater, the circulating current will be higher, and conversely.

2. Choice of Frequency

RF systems of early e^+-e^- storage rings operated at frequencies below 100 MHz; the SPEAR I RF system, for example, operated at a frequency of 51 MHz. Although operating at this low a frequency does have some important advantages, the shunt impedance per unit length of the cavities is on the order of only 1 MΩ/m. If the PEP RF operating frequency were chosen to be at such a low value, then the RF structure would need to be several hundred meters in length in order to attain the high peak voltage required. By using a higher frequency, as in SPEAR II, the geometric shape of the cavities can be optimized without introducing unduly large structures, and the shunt-impedance-per-unit-length can be increased significantly. The disadvantage in using a higher frequency is that the overvoltage ratio (peak voltage divided by the synchrotron radiation loss per turn) required to give a reasonable quantum lifetime also increases. Taking these two competing factors into account, it can be shown that there is a rather broad optimum for PEP in frequency region 100 to 400 MHz,[23] but biased toward the lower end of this range if parasitic-mode losses are also taken into account.

Given this optimum frequency region, then economic and engineering considerations dominate the choice of RF frequency. The structure diameter, weight, and cost increase as frequency decreases. The same is true of the available RF power sources. A careful study of the comparative advantages of klystrons vs gridded tubes was made in connection with the design of the RF system for SPEAR II.[24] It was concluded that klystrons were superior to available gridded tubes with respect to initial and annual operating costs, reliability, and expected life. Klystron size and cost are lowest at the upper end of the 100-400 MHz frequency range. These factors led to a choice of 358 MHz for the SPEAR II RF system, and similar reasoning leads to the conclusion that a frequency of 353 MHz is reasonable for PEP. This choice has the added significant advantage that the successful SPEAR II RF system becomes a model for the PEP system.

The 358-MHz SPEAR II RF system is described in Ref. 25. Installation was completed in November 1974, and operation is now routine. Colliding beams have been obtained up to 4 GeV, where the peak accelerating voltage is over 6 MV. Some of the problems encountered and the measures taken to resolve them are discussed in Ref. 25. So far they do not indicate any basic reason why this system cannot be extended to meet the PEP requirements. In summary, we feel that the experience obtained from the construction and operation of the SPEAR II RF system provides a firm basis for the design of the PEP system.

3. Structure Design

The requirement of cw operation at high energy gain, together with the need in a storage ring to minimize the space occupied by the RF system, demands an RF structure with high shunt-impedance-per-unit-length. Thus, many

of the same considerations entering into the design of the shaped-cavity LAMPF accelerating structure[26] also apply to the PEP structure. There are in addition some further special design considerations. These include the large aperture required to accommodate the storage-ring beam during injection, the need for tuning to compensate for reactive beam loading and for thermal detuning effects, and the requirement to mask some surfaces against intense synchrotron radiation. In addition, in a high-energy storage ring the RF power transferred to the beam per unit length of accelerating structure is typically much higher than in linacs. In the PEP case, for example, it may reach 100 kW/m. Taking these factors into consideration, the accelerating structure chosen for SPEAR II consists of five strongly coupled cavities operating in the π mode so as to accelerate both counterrotating beams. This structure is depicted schematically in Fig. 31 and a photograph of an accelerating section is shown in Fig. 32. The shape of the individual cavities has been adjusted to produce a high shunt impedance which, for a perfect copper surface, would be 30 MΩ/m. The coupling slots reduce this figure by about 10%. In addition, an aluminum alloy having a surface conductivity 75% that of copper was used in the fabrication of the SPEAR II cavities. Taking into account the fact that surface conductivity for real surfaces falls 5 to 10% below the theoretical predictions, a shunt-impedance-per-unit-length of about 19 MΩ/m was predicted for the SPEAR II structure. This value was confirmed both by cold test measurements and by performance in the SPEAR ring.

Modifications will be required to adapt the structure to PEP operating conditions. Of particular importance, the higher power density per unit length (a maximum of 100 kW per cavity) will require increased cooling. The nose cones, for example, will be shortened to provide shorter heat paths. Simplifications

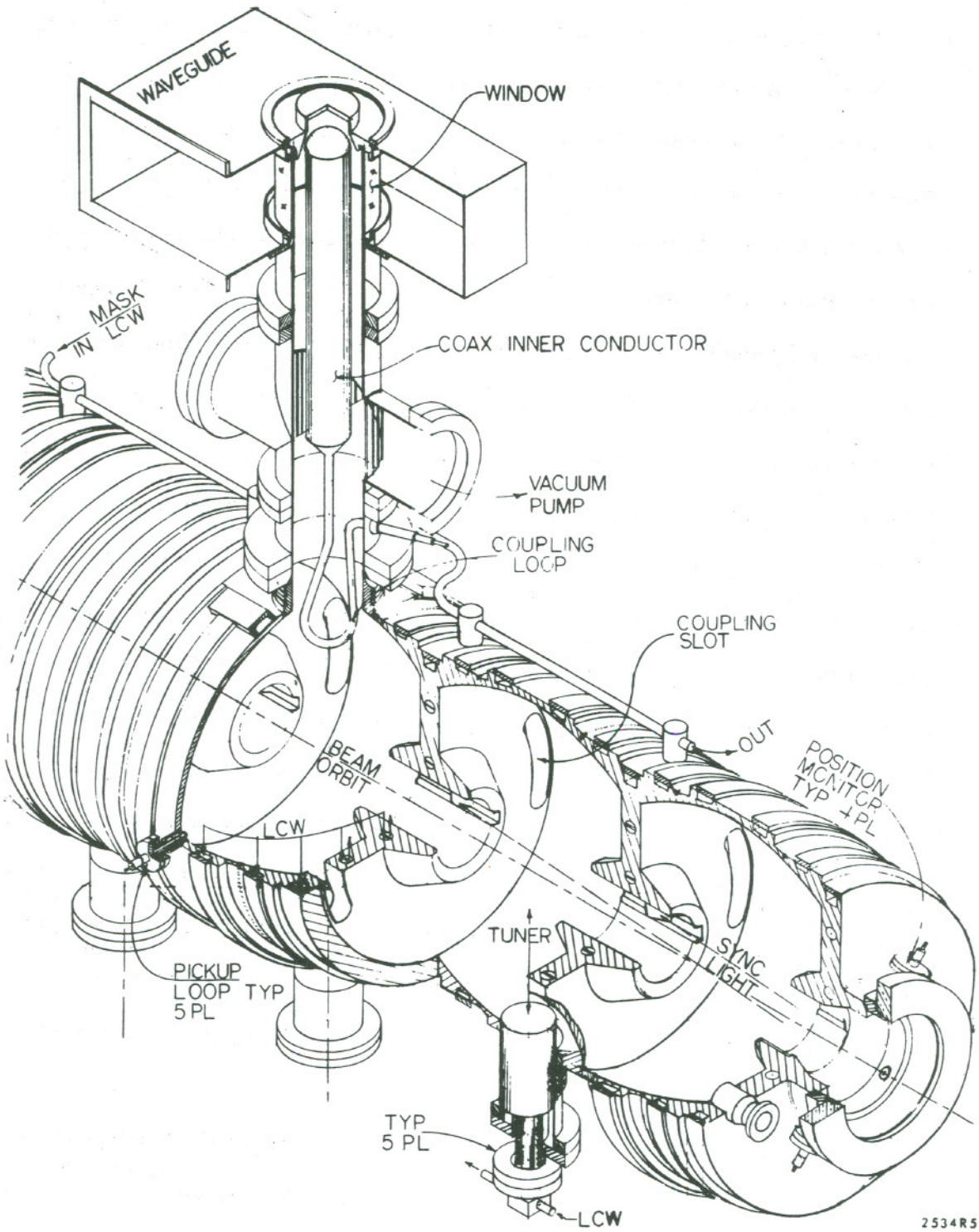

Fig. 31--Cutaway view of the SPEAR II accelerating structure.

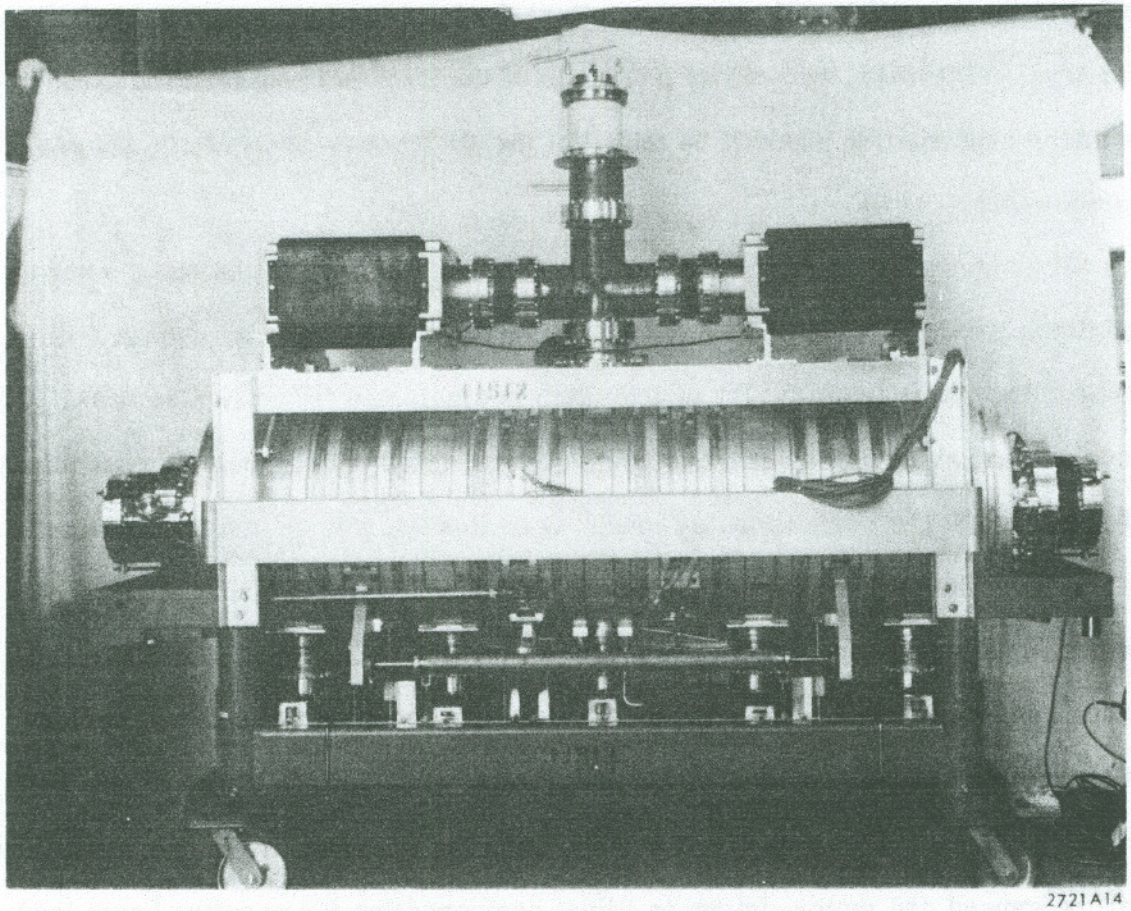

Fig. 32--Photograph of the SPEAR II accelerating structure.

will also be made in the cavity shape to permit easier fabrication. A 1/7-scale model has been built and measured as part of the PEP R&D program, and the results of these measurements indicate that there is a loss of about 13% in shunt impedance due to these modifications. On the other hand, a 1100-series aluminum alloy having higher thermal and electrical conductivities will be used in the fabrication of the PEP structure and the gain in RF conductivity (about 16%) in going to the new alloy will more than offset the loss due to changes in cavity geometry. A full size, two-cavity prototype of the modified accelerating structure is under construction and will be tested at the PEP power level of 100 kW per cavity early in 1976.

The unloaded Q of this structure will be about 30,000. At 15 GeV, where a maximum beam current of 92 mA (each beam) will be stored, the beams will extract more power from the RF source than is dissipated in the cavity walls. The accelerating structure must therefore be overcoupled with a coupling coefficient of about 2.5. The corresponding loaded Q is about 8,000 and the filling time is 7.5 μsec. The peak voltage which would be induced by the beam if all 18 accelerator structures were tuned to resonance would be about 37 MV for two circulating beams of 92 mA each. Each cell of the five coupled cells in an accelerating section will be provided with a separate tuner. Initially these tuners will be hand-adjusted to compensate for manufacturing tolerances. In operation they will be ganged and motor-driven to adjust compensation for reactive beam loading and provide stability against phase oscillations.

4. Klystrons

The need for klystrons capable of supplying 500 kW of cw RF power at 353 MHz can be met with several designs. It would be easiest simply to scale the SPEAR II klystrons, which have demonstrated an efficiency slightly greater than

55% at a power output of 125 kW. If this were done, the dc input power to each klystron would be close to 1 MW. However, in view of the scarcity and cost of power, both now and to be expected in the future, it is especially desirable to develop a very high efficiency klystron to reduce the total power consumption for the PEP RF system. Computer calculations indicate that an efficiency somewhat greater than 70% should be achievable in a 500-kW tube. The input power per tube would then be 715 kW instead of 910 kW, reducing by 3.5 MW the total installed capacity for the 18 stations. Such high efficiency is achieved by introducing a second-harmonic cavity which, at the fundamental frequency, produces sharper bunches having a greater component of RF current at the output cavity. This requires additional interaction length, and results in a klystron which is about four meters long.

An experimental tube has been built. A schematic diagram of it is shown in Fig. 33 and a photograph in Fig. 34. This experimental tube is at present being tested under pulsed conditions since it does not have a full-sized collector. In initial tests we have measured an efficiency of 63% with 60 kV on the anode. A power output of 500 kW was reached at 65 kV. The measured gain was within 1 dB of that predicted by the computer design program. By reshaping the profile of the magnetic focusing field along the tube axis, we expect that the efficiency can be increased further, approaching the design value. A full-scale klystron capable of cw operation at the 500-kW design level will be ready for testing in the spring of 1976.

Typical parameters of the PEP klystron operating into a matched load are:

Beam Voltage	62	kV	Drive Power	15	W
Beam Current	11.5	A	Output Power	500	kW
Beam Power (input)	713	kW	Electromagnet Focusing at 25 A	50	V
Frequency	353	MHz			

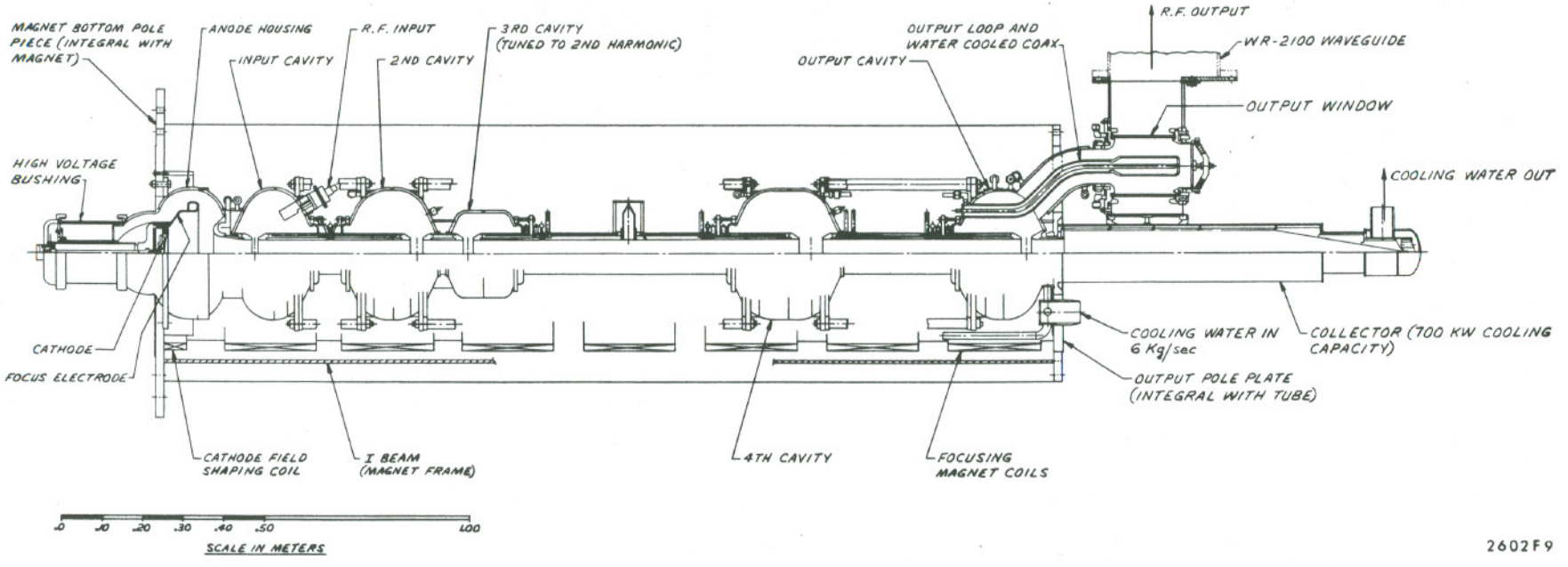

Fig. 33--Schematic diagram of the experimental PEP klystron.

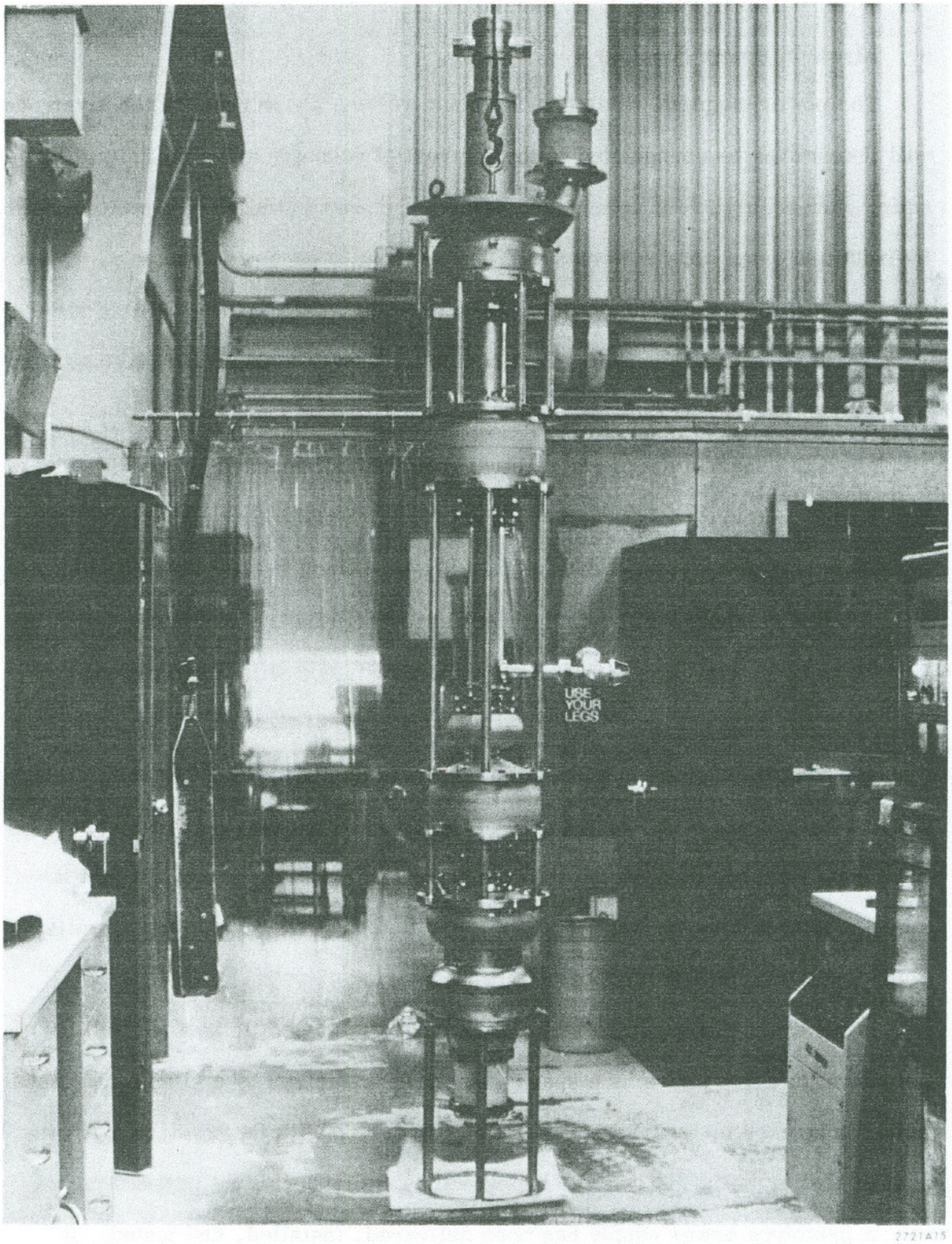

Fig. 34--Photograph of PEP prototype klystron.

5. Klystron Power Supplies

The power supplies which provide beam voltage and current to the klystrons will themselves be unregulated in the interest of economy and simplicity. However, slow regulation of voltage and adjustment over a limited range is afforded by induction regulators in series with the ac input to each power supply. These low-priced, commercially available units provide voltage control over a 20% range in 5/8% steps (Fig. 35). Fine control of the RF accelerating voltage can be obtained by varying the RF drive to the klystrons.

Since the characteristics of all klystrons will not necessarily be identical, taps on the primaries of the high-voltage transformers will permit the optimum operating voltage to be selected for each klystron when it is installed and as its characteristics change with aging. Each supply will have a maximum output of 756 kW at 63 kV and 12 A. They will be oil-filled units with a solid-state rectifier and a 6-henry filter choke contained in the same oil tank. They will be in weatherproofed housings located outdoors, as indicated in Fig. 30, minimizing the fire hazard and reducing the size of the klystron buildings. The output of each supply passes through the building wall to a high-voltage cabinet just inside, housing a one-microfarad filter capacitor, crowbar, interlock circuits, control circuits, and voltage and current metering circuits.

In the event of a klystron fault, the energy dissipated in the fault will be held down to a few joules by a spark-gap crowbar, driven by a simple thyratron pulser triggered by a current transformer in series with the klystron. A vacuum contactor at the input to the supply will simultaneously be tripped.

A prototype power supply has been delivered, installed, and tested. It will be used first in tests on a diode composed of the gun and collector from the 500-kW tube. These initial tests will, in addition to proving the capability of

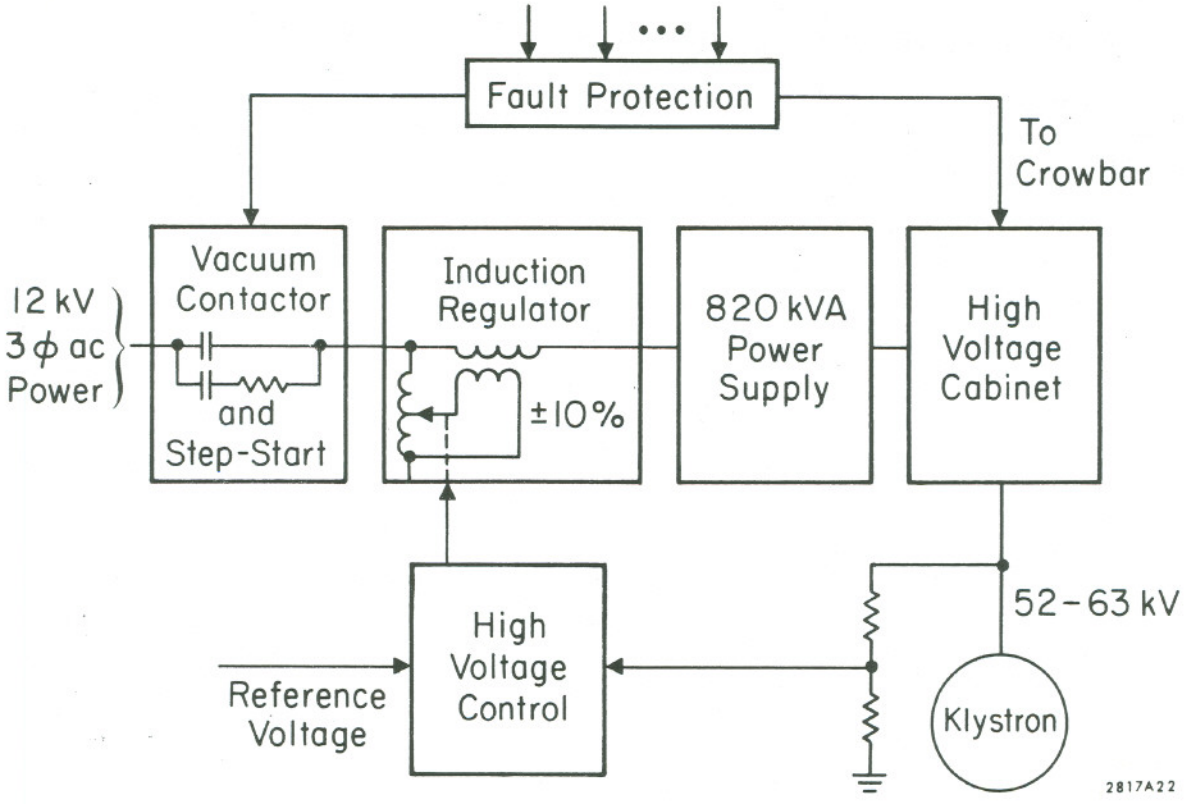

Fig. 35--Klystron power supply block diagram.

the power supply, provide a test of the gun and collector design for the full-scale tube. Tests on the first full-scale model klystron will follow.

6. Phasing and Tuning

A block diagram showing the drive, phasing, and cavity-tuning systems for the RF system is given in Fig. 36. Consider first the control system for accelerator section tuning which must be adjusted with increasing beam current. A phase bridge will accomplish this by comparing the phase of the RF power incident on the accelerator section with the phase of the field in the section. The output of the phase bridge activates the tuner drive, which moves the tuners either in or out to null the signal from the phase bridge.

Relative phasing of the accelerating sections will be carried out by first capturing a low-energy beam in the ring with a single RF cavity on. Then a second cavity will be turned on and phased relative to the first by maximizing the synchrotron oscillation frequency. This second cavity will then be turned off and a third one turned on and phased to the first in a similar manner and so on, until all the cavities have been successively phased.

In operation of the system the largest changes tending to degrade the phase alignment will be phase changes across the klystron as the beam voltage and klystron drive are varied. A phase-lock loop around the klystron will reduce these changes to acceptable levels. A stable phase reference cable will carry phase information from a pickup in each accelerator section back to a phase bridge near the RF source. At any time, the phase can be touched up to within an accuracy set by the stability of the phase reference cable by varying the input phase to each klystron until the phase of the signal from each cavity pickup agrees with a reference phase setting. The reference phase settings are those measured for each pickup immediately after the complete phase alignment has

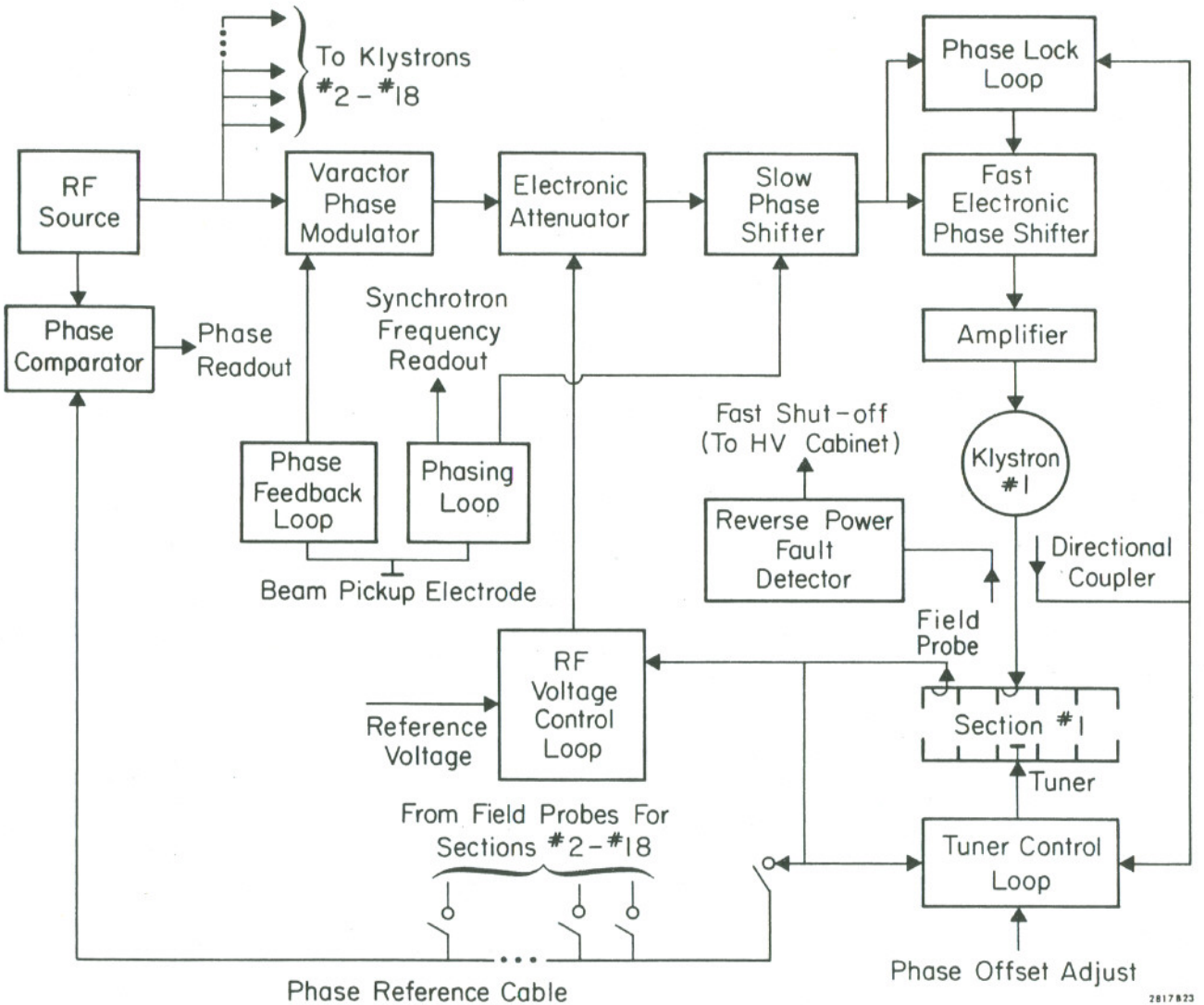

Fig. 36--Block diagram of the drive, phasing, and cavity-tuning system.

been made using the synchrotron-frequency technique described above.

7. Control of Longitudinal Instabilities

The six circulating bunches in PEP can be considered as six coupled harmonic oscillators with six normal modes. The inphase barycentric (zero-mode) phase oscillations of the bunches can probably be stabilized by appropriate tuning of the accelerator sections. Should this measure prove to be inadequate, this mode can be controlled by a feedback loop using a narrow-band phase signal picked up from the beam and fed back to phase modulators in the input drive lines to the klystrons. In order to damp the other five possible modes, one or more high-frequency cavities may be required. When such cavities are in operation, the time derivative of the voltage, and hence the synchrotron oscillation frequency, is different for each bunch. If this "splitting" of the synchrotron frequencies is sufficiently large, the bunches are effectively decoupled against longitudinal phase oscillations. This technique proved successful in SPEAR I and in other storage rings. In SPEAR II, however, no longitudinal phase oscillations of any kind are normally observed, leading us to expect that they may not occur in PEP. For this reason high-frequency cavities will not initially be installed in PEP, although provision will be made for them should the need be demonstrated.

Three potential longitudinal instabilities which can arise out of the beam-beam interaction have been suggested and studied.[27] They appear not to be significant for PEP. The first instability occurs only when the colliding beams cross at an angle, which is not the case in PEP. The second one is due to a nonzero value of η^*, the η-function at the interaction region. It places an upper limit on η^* which is higher than the value at which PEP will operate. The third instability occurs when the bunch length is large compared to the value of the β-function at the interaction region. This again will not be the case in PEP.

8. Loss to Parasitic Modes

As discussed previously, parasitic modes in the RF cavities and in vacuum chamber components lead to an additional loss of energy from the beam particles over and above that due to synchrotron radiation. Both theoretical and experimental approaches have been used to estimate the magnitude of this loss for the PEP design. Calculations are available which give the loss for the case of a closed cylindrical box, or for the case of a chain of such boxes coupled by holes on the beam center.[28] To the extent that such a disk-and-cylinder model can predict the higher mode losses for the PEP RF structure, these losses follow the relation $R(CAV) = 110 \exp(-0.43\,\sigma_z)M\Omega$ for the 90-cavity structure proposed for PEP, where R is the higher mode loss resistance and σ_z is the bunch length in cm.

An experimental measurement on SPEAR II gives an indication of the losses that might be expected for the "incidental" vacuum chamber cavities.[29] By subtracting the calculated higher mode losses for the RF cavities from the total measured loss for SPEAR II, an expression is obtained for the vacuum chamber loss alone. This loss, when scaled to the PEP circumference, assuming the same loss per unit length of vacuum chamber as in SPEAR II, gives $R(VAC) = 915 \exp(-0.3\,\sigma_z)M\Omega$. However, in designing the SPEAR vacuum chamber, no effort was made to reduce the number or magnitude of the discontinuities which determine the parasitic mode loss. After reviewing the construction of the SPEAR vacuum chamber, it was felt that it was not unreasonable to expect that these losses could be reduced by a factor of 10. Adopting this as a criterion, we add one-tenth of the vacuum-chamber loss obtained from the preceding expression to the calculated loss for the RF cavities and a total parasitic mode loss of $R(TOT) = 200 \exp(-0.36\,\sigma_z)M\Omega$ is obtained for PEP.

Using this expression for parasitic-mode loss, the circulating current for PEP can be calculated as a function of energy. The calculation is described in detail in Ref. 30 and uses parameters appropriate to the lattice described previously in Section II. A. Results are shown in Fig. 37 for three different lengths of RF structure. The solid line gives the stored current capability for the 38 m long structure proposed for initial installation. Results are also shown for RF structure lengths which are twice and four times as long. In all three cases the stored current capability is 92 mA or more at 15 GeV; the advantages of the longer systems lie in a savings in RF power at 15 GeV and below and a higher stored-current capability above 15 GeV. For a stored current of 10 mA per beam, the energies reached by the 38 m, 76 m, and 153 m systems are seen to be 18.0 GeV, 19.8 GeV, and 21.6 GeV, respectively.

All stored currents shown in Fig. 37 have been calculated for bunches which are lengthened by a fixed factor of two over the natural bunch length, which is the estimated bunch lengthening at the design current level. At lower currents, the actual bunch lengthening will probably be less, the parasitic-mode losses will be somewhat greater, and the stored currents will be slightly less than shown.

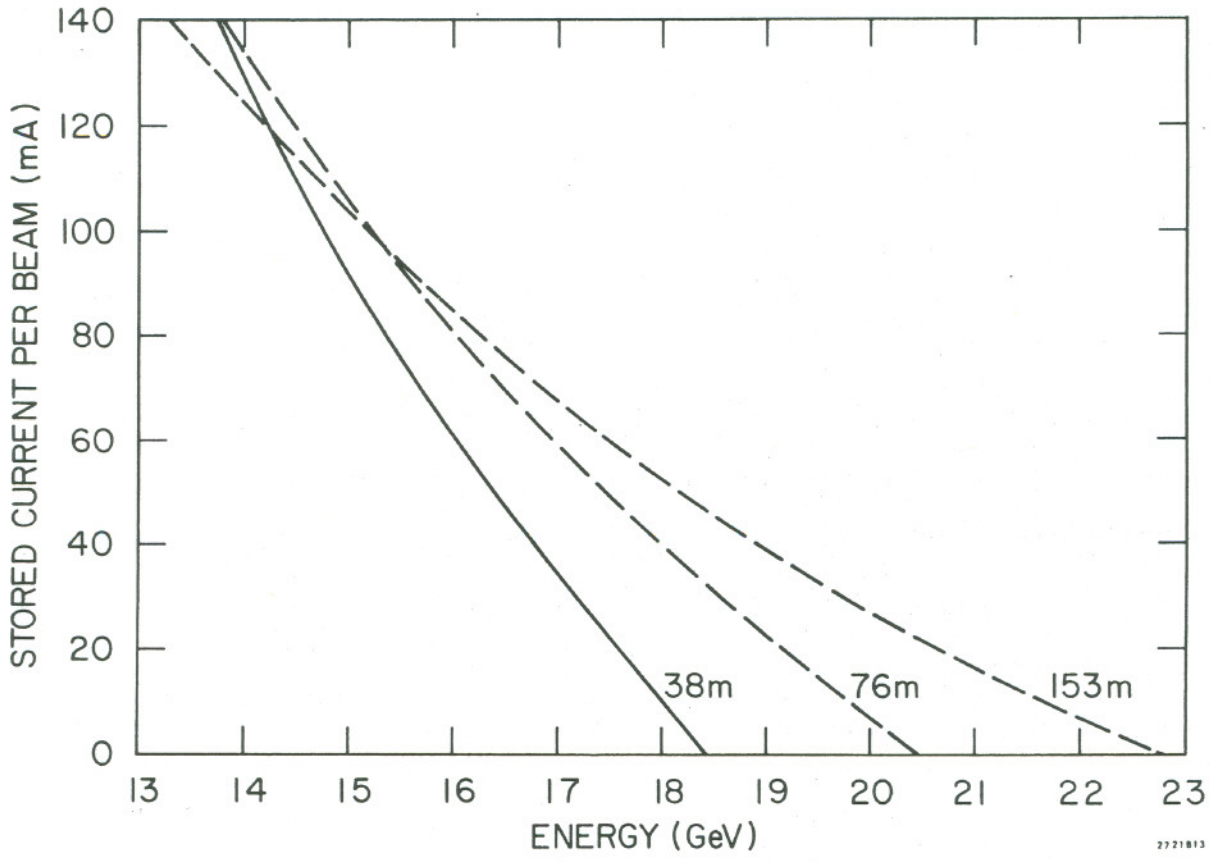

Fig. 37--Stored current per beam for several lengths of RF structure.

D. Vacuum System

1. Introduction

The vacuum system proposed for the PEP storage ring will be similar to the successful SPEAR design, which has proven so reliable and satisfactory, both in construction and operation.[31] Any modifications are due primarily to the increased synchrotron power radiated per unit length, which tends to increase radiation-induced gas desorption. All design parameters and system features are dictated by the pressures required to achieve adequate beam lifetimes and acceptable background rates in the interaction region areas.

2. Vacuum Chamber Construction

The vacuum chamber in the bending magnets will be 14 meters long (Fig. 38), of extruded 6061-T4 aluminum with an internal cross section as shown in Fig. 39. The inner cross-sectional area is designed to accommodate the beam-stay-clear region required by beam dynamics and to allow for unavoidable errors in mechanical positioning. The synchrotron-radiation-absorbing wall will be approximately 10 mm thick. As shown in Fig. 38, a regular cell contains one bent aluminum extrusion and one instrument module. The stainless steel instrument module will accommodate an expansion bellows, position monitors, vacuum gauges, synchrotron radiation masks, holding pumps, and other components.

The segments of the vacuum chamber are joined together with standard vacuum flanges, all of which will be of stainless steel with copper gaskets. The largest flanges are the holding pump flanges and the 250-mm flanges at the ends of the chambers. They will be attached to the aluminum chambers by means of transition sections made of the explosively bonded aluminum-stainless steel sandwich material used in SPEAR, where the system has reached base

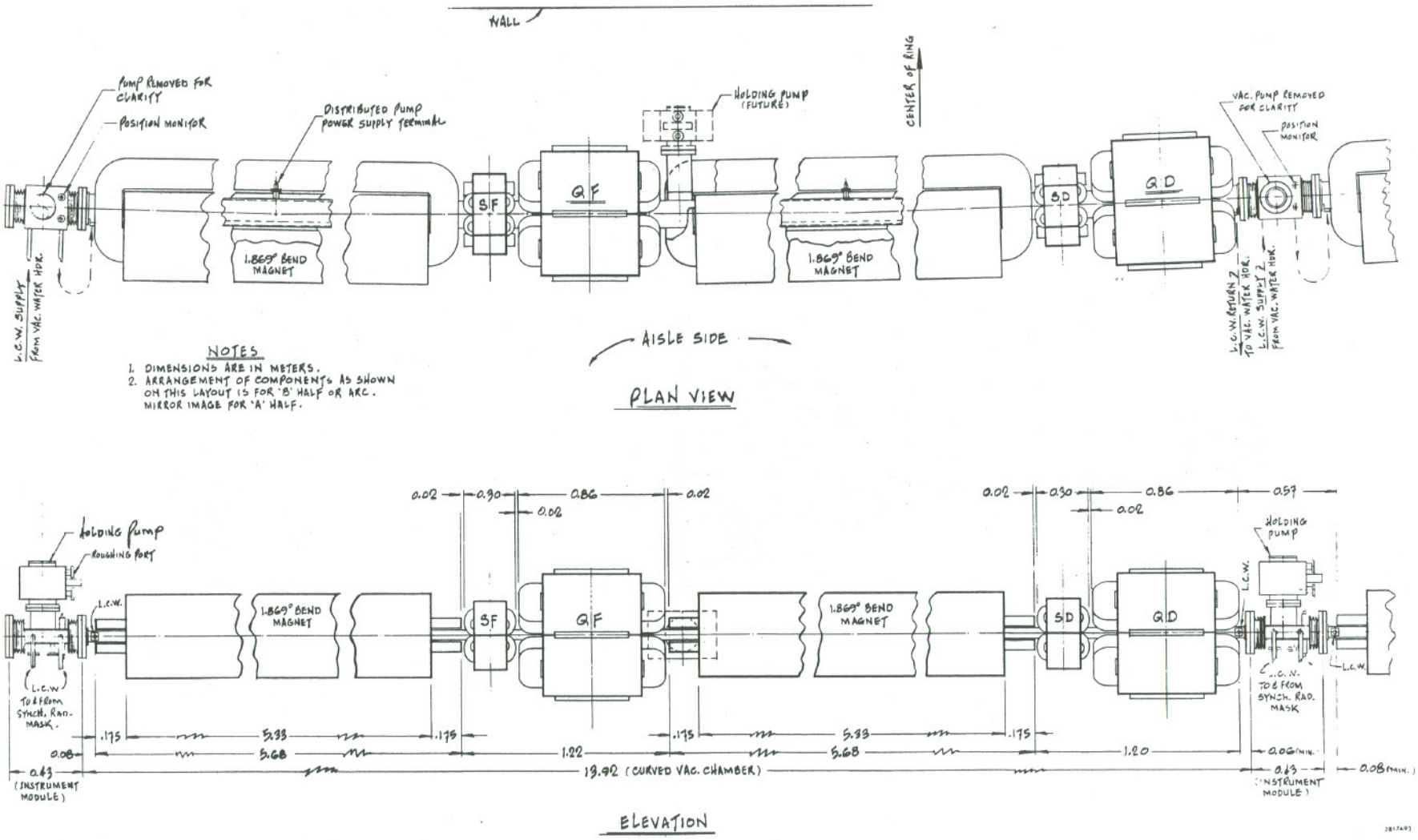

Fig. 38--Standard cell bend vacuum chamber module.

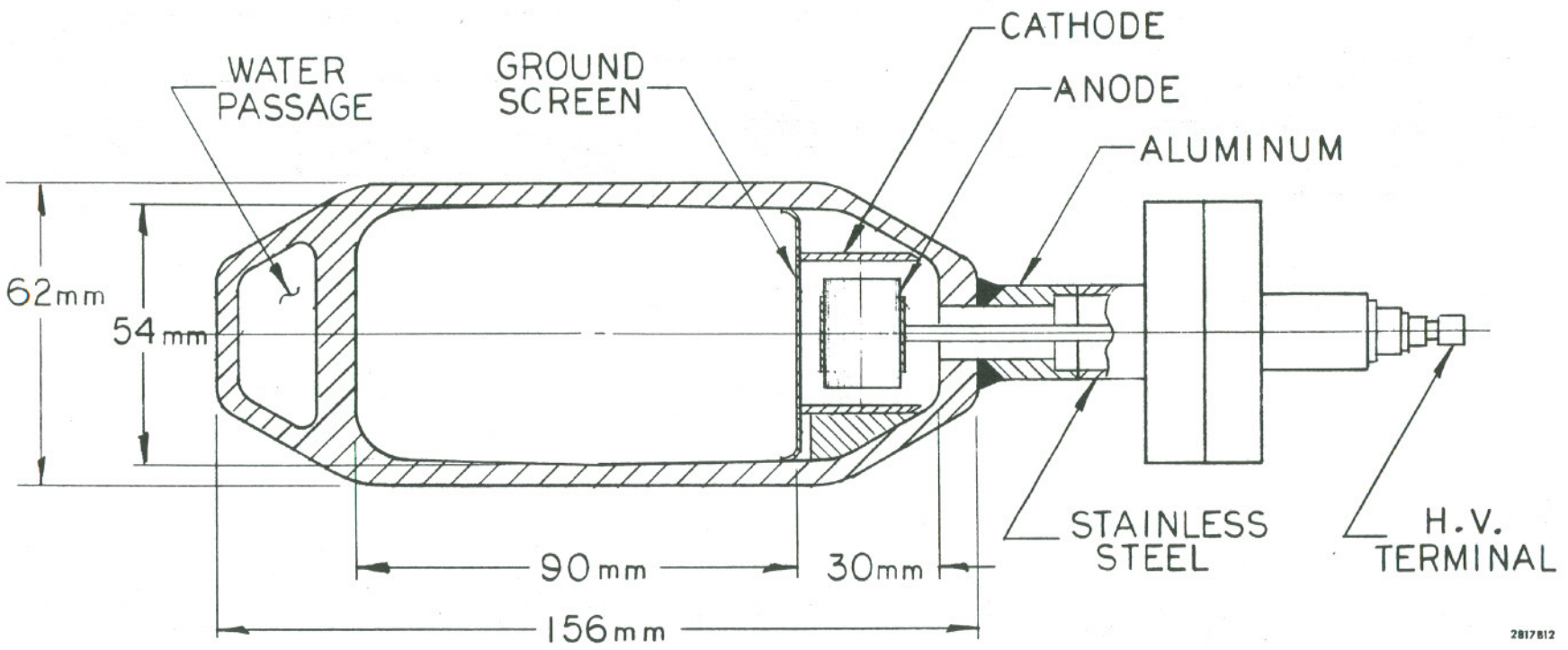

Fig. 39--Cross section of bend magnet vacuum chamber.

pressure levels lower than 2×10^{-10} Torr without any in-place bakeout and with no detectable leaks.

In view of the concern regarding the higher-order-mode losses evidenced at SPEAR,[29] changes and discontinuities in vacuum chamber cross section will be held to a minimum. The individual sections of vacuum chamber will be continuous through two bend magnets and two quadrupoles, and mesh screens will mask the beam from unavoidable abrupt changes in chamber cross section, caused, for example, by bellows and pump ports.

3. Synchrotron Radiation

The spectral energy distribution of the synchrotron radiation is shown in Fig. 40. The critical energy at 15 GeV is 45.4 keV with a considerable fraction of the photons having energies above 80 keV. In the region below 40 keV, the photoelectric process dominates the attenuation of photons in aluminum; hence almost all the power at these photon energies is absorbed in the chamber wall. Above this photon energy, attenuation by Compton scattering begins to dominate. Calculations show that many of these photons are scattered out of the chamber wall with energies above 3 keV carrying away about 40% of the radiated synchrotron power.

One of the major factors determining the vacuum system design is the thermal load which must be dissipated by surfaces subject to intense synchrotron radiation. Design criteria must be conservative to reduce the danger of a burnout, and a resulting water-to-vacuum leak. Therefore, for design purposes of the PEP vacuum system, we assume that all the synchrotron power is absorbed in the walls and masks even though some escapes the system.

At 15 GeV with 92 mA stored in each beam, the total power radiated per beam will be 2.5 MW. The design power distribution for the vacuum chamber

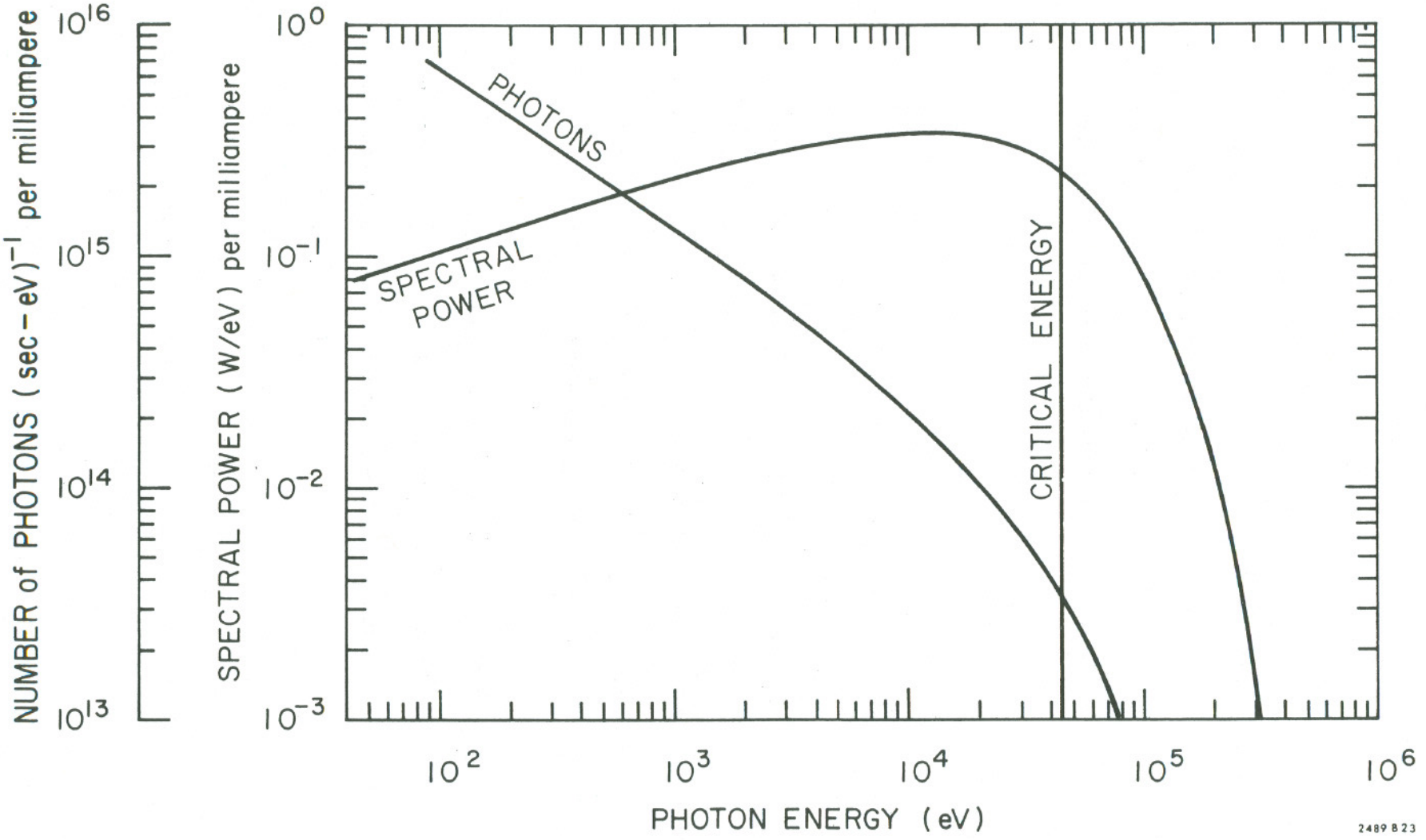

Fig. 40--Photon and power spectrum of the synchrotron radiation at 15 GeV.

geometry in a main bending cell is plotted in Fig. 41. The maximum linear heat flux for two counterrotating beams is about 46 W/cm. These values include a 10% margin for safety above the total radiated power.

Heat fluxes in the zones adjacent to the wiggler magnets will be particularly high, the maximum being 115 W/cm as shown on Fig. 42. This flux is based on a maximum synchrotron radiation power loss of 141 kW/beam, for each of the wiggler triplets required for beam size control. See Fig. 10. Special absorbers will be required in these regions.

The main gas load is due to synchrotron-radiation-induced desorption, which is a function not only of the machine energy and stored current, but also of the condition and history of the irradiated surface. The crucial measure of gas desorption is the pressure rise when beams are stored in the ring. When the first beams are stored, the initial rise will carry the pressure two or three orders of magnitude above the base pressure. Continuous exposure to synchrotron radiation will "condition" the surfaces and then the pressure rise will decrease. The total synchrotron-radiation-induced gas load for the storage ring is estimated by extrapolation from SPEAR to be on the order of 10^{-5} Torr ℓ/mA-sec at 15 GeV, after a reasonable period of conditioning.

4. Vacuum Pumps

The vacuum system is conductance-limited in the bending-magnet chambers, where most of the outgassing occurs. Here, we will use the same type of distributed sputter-ion pumps developed and used for SPEAR. These pumps are rated at 160 ℓ/sec per meter of pump length. Commercially available 100 ℓ/sec ion pumps will be mounted at every second quadrupole, and will maintain the system at a base pressure of 1×10^{-9} Torr without a stored beam.

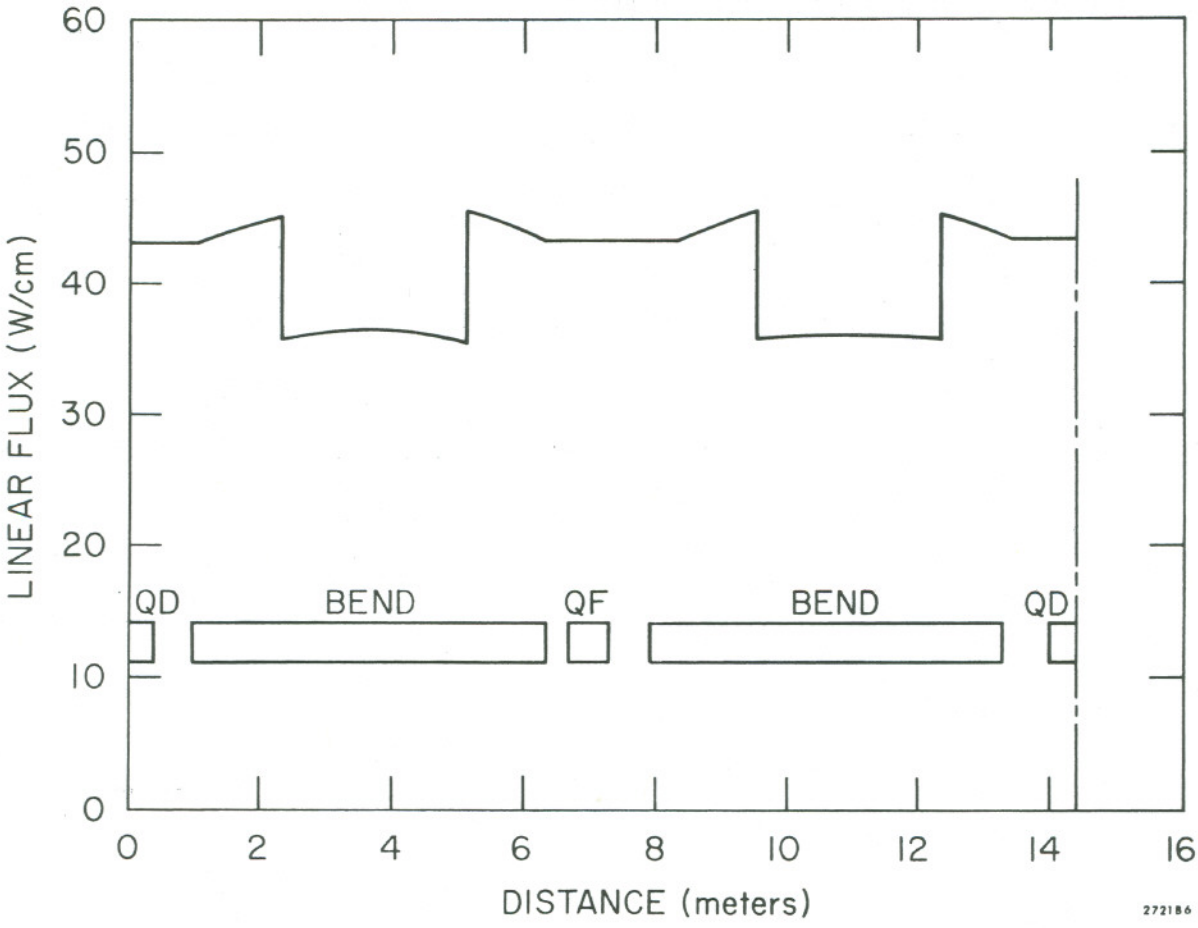

Fig. 41--Synchrotron radiation power distribution in a cell at 15 GeV.

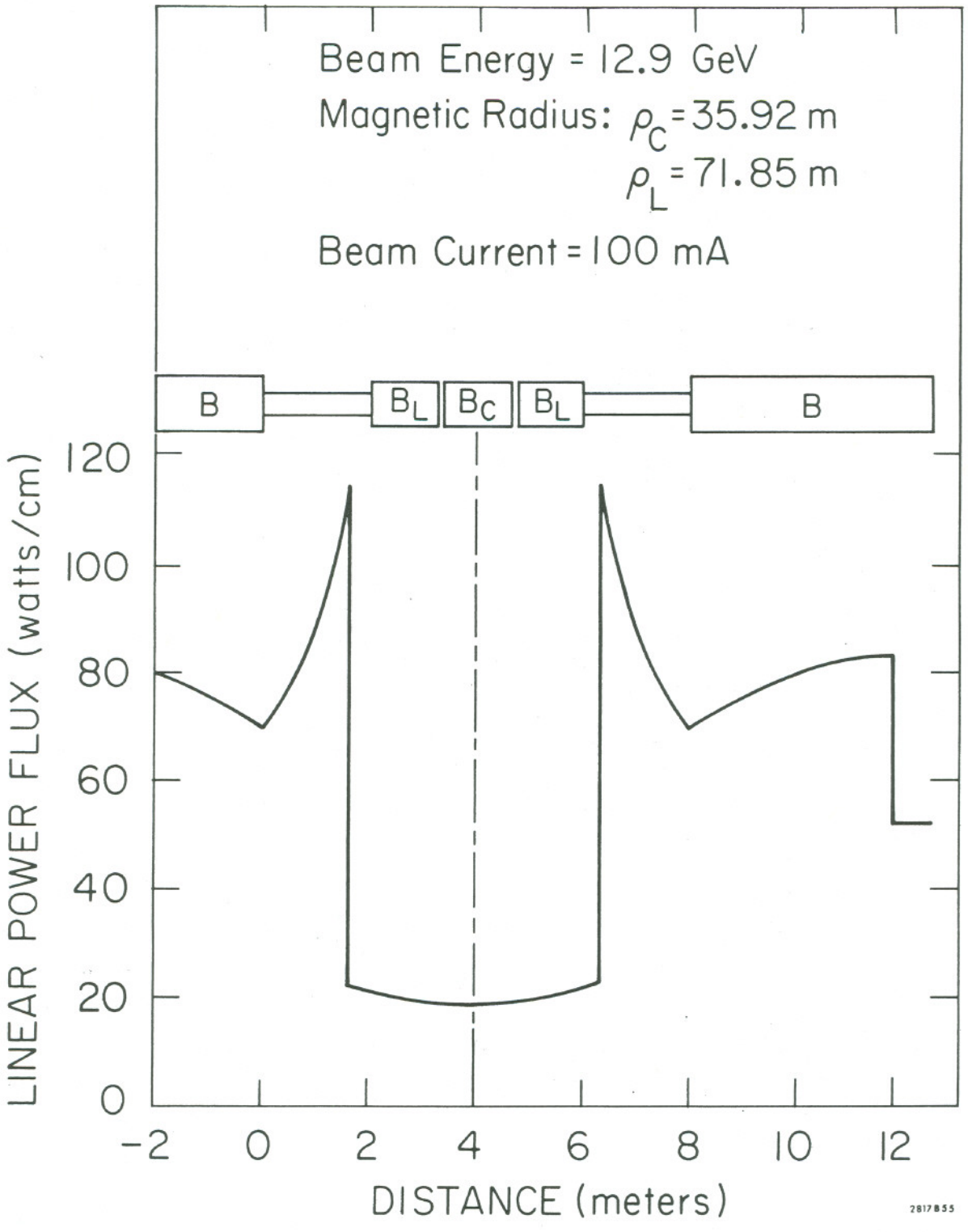

Fig. 42--Synchrotron radiation power distribution in the wiggler magnets.

With two 15-GeV, 92-mA beams circulating, the calculated pressure distribution is as shown in Fig. 43. Based on the above estimate for the total gas load, the average pressure will be on the order of 2.2×10^{-8} Torr. We are studying the possibility of future installation of additional 100 ℓ/sec pumps, to reduce the average pressure to 1.0×10^{-8} Torr. See Fig. 43.

5. Instrumentation, Valves, Controls, etc.

Isolation valves, vacuum gauges, and blanked-off pump ports are incorporated in the design to make pumpdown easier, to isolate sections as protection against accidental venting-to-air, and to facilitate diagnostics. There will be a nude pressure gauge in every fourth cell. Four inline, all-metal valves will be installed in each arc and can be actuated manually, either locally or from the Control Room, or automatically upon any indication from the vacuum gauges of abnormal pressure rise. Ports with all-metal right-angle valves will be installed in each instrument module. They will be used for pumpdown connections, installation of mechanical or thermocouple gauges, diagnostics, and venting. Pumpdown will be accomplished by a combination of trapped mechanical pumps and cryosorption pumps.

6. Cooling Water

Based upon the distribution of synchrotron radiation per cell as shown in Fig. 41, the maximum heat flux is 46 watts/cm. The temperature differential across the water-cooled wall of the chamber at this flux is approximately 45°C, and the temperature differential across the surface film in the water is 26°C. Water will be supplied at 30°C and the total water flow for the storage ring will be 220 ℓ/sec to hold the bulk temperature rise to 10°C.

The thermal conditions given above determine the thickness of the water-cooled web of the vacuum chamber and the area of the cooling water passage.

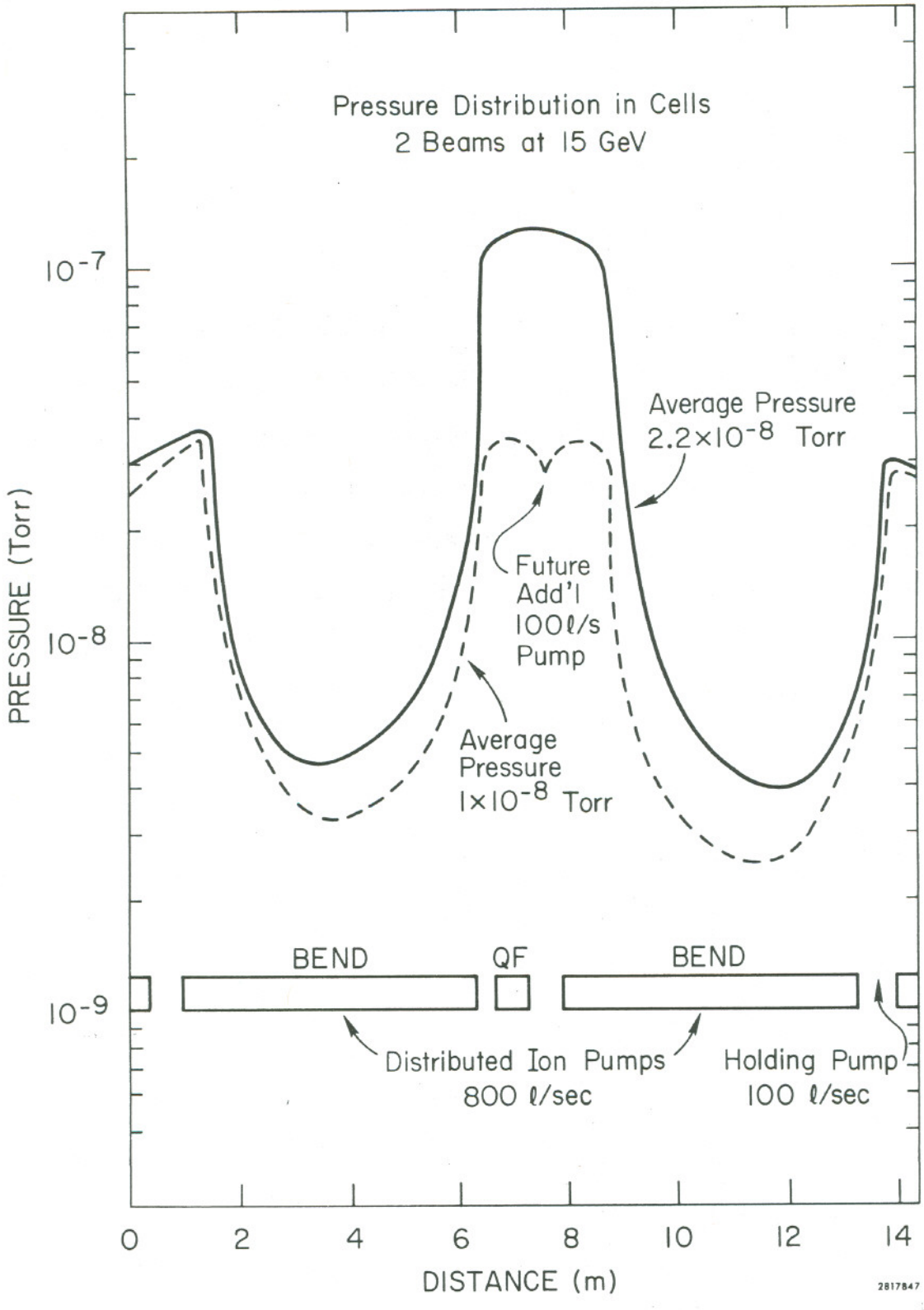

Fig. 43--Gas pressure distribution in a cell at 15 GeV.

A supply-water pressure of 17 atm, with a differential pressure drop of 13 atm through the fourteen meters of cooling water passage, will provide the flow without exceeding the allowable stress in the cooled web.

Figure 44 shows a conceptual design of the instrument module, which includes the pump port, position monitor, synchrotron-radiation mask, and ports for pumpdown and instrumentation. The copper mask, brazed to the stainless steel cooling tubes, will average 3 cm in thickness. For the configuration shown, the maximum local water temperature will be less than 100^{o}C, and the maximum local metal temperature will be less than 250^{o}C.

Due to the intense heat fluxes and the associated heat transfer problems, the vacuum chamber cooling water system must be an independent high-quality system.

7. Insertions

The vacuum chambers for the insertion regions will be fabricated mostly from 300-series stainless steel tubing. The initial design of the insertions, where, in contrast to the arcs, the main gas load is due to thermal outgassing, will provide for an average pressure of 5×10^{-9} Torr, primarily of gas with mass 28. The chambers will be provided with ports to simplify the addition of pumps adequate to maintain an average pressure of 5×10^{-10} Torr of mass 28 gas if experimental conditions require it.

Experience at SPEAR has shown that a large number of high-energy photons can be scattered or transmitted into the interaction areas requiring collimators to shield off extremely high backgrounds. To abet the low-field magnets and the bend magnets already mentioned in Section II.A.9, a pair of high-Z masks, one movable and the other stationary, will be located at the entrance of each interaction region. These masks will be water-cooled.

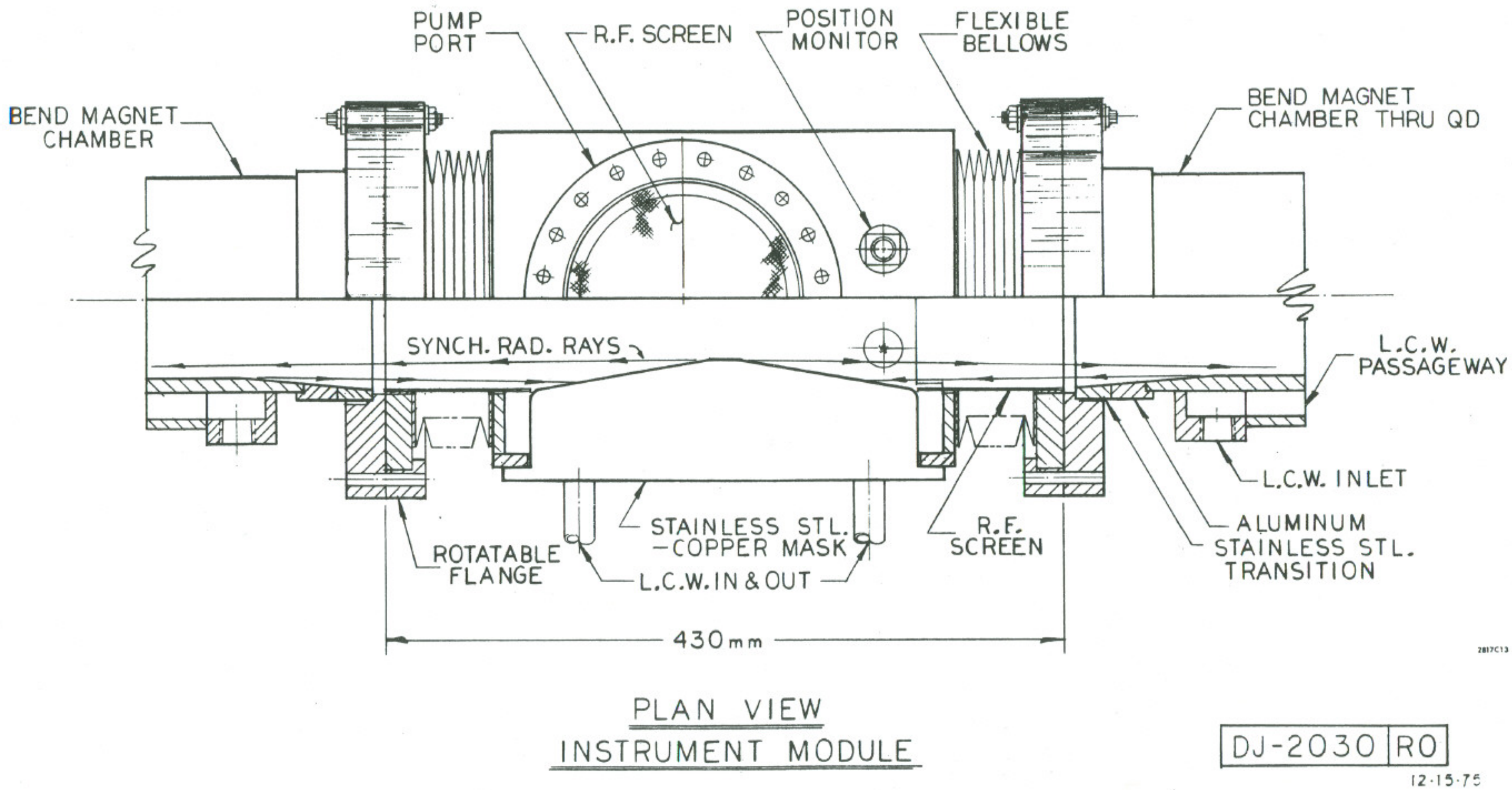

Fig. 44--Conceptual design of the instrument module.

8. Bakeout

The extruded aluminum vacuum chambers in the arcs will be baked out by circulating hot water (185^{o}C) through the cooling water passages. The bakeout mantle for the chambers will consist of 4 mm of insulating material covered with glass tape and insulating paint. Calculations show that the transverse temperature difference across the width of the chamber will be 18^{o}C and the water flow required for the bakeout will be one ℓ/sec per chamber at 185^{o}C and 18 atm. All chambers will be baked to a temperature of 185^{o}C to 200^{o}C prior to installation in the ring.

The instrument-module chambers and the chambers in the insertions will be wrapped with electrical heater tapes and sufficient insulation to achieve a bakeout temperature of 200^{o}C. Bakeout temperatures will be monitored by the use of remotely read thermocouples.